

Application of wavelet fractal algorithm to feature extraction of hydro-turbine vibration signals

X. ZHIHUI^{a,*}, C. YUFAN^a, Y. YANAN^a, O. P. MALIK^b

^aWuhan University, School of Power and Mechanical Engineering, Wuhan 430072, China

^bUniversity of Calgary, Department of Electrical and Computer Engineering, University of Calgary, Canada

To avoid the drawbacks of traditional fractal theory, such as complicated calculation and the difficulty in choosing the proper kind of fractal dimension, a wavelet fractal algorithm is proposed in this paper for the feature extraction of a hydro-turbine vibration signals. In this algorithm, wavelet functions are used to decompose the de-noised signal. After decomposition, variance of each level of the detailed components is introduced to describe the energy distribution on each level. The fractal dimension is the slope of the fitting line by taking scale j as the horizontal axis and variance as the vertical axis. To verify the theory introduced in this paper, a comparison of the wavelet fractal algorithm with the conventional fractal algorithm on a few sets of experimental vibration signals shows that although both methods are successful in feature extraction, the wavelet fractal algorithm provides more accurate feature extraction of hydro-turbine vibration signals.

(Received October 23, 2014; accepted January 21, 2015)

Keywords: Fractal dimension, Correlation dimension, Wavelet fractal algorithm, Hydropower vibration signals

1. Introduction

Hydro-turbine is an important component in electric power generation. A fault in such a device could lead to huge economic losses and, therefore, it is desirable to conduct correct and efficient fault diagnosis on this facility. Fault diagnosis is performed when a hydro-turbine is malfunctioning. It can be used to determine the cause(s) responsible from a set of observed symptom(s). Vibration signals contain abundant information on the operation status of the mechanical equipment, and its analysis is of significance to the fault diagnosis of rotating machinery, including hydro-turbines. Generally, the analysis of vibration signals can be divided into two aspects: one is to further understand the fault mechanism, and the other is to extract effective features for fault diagnosis. Many techniques, like traditional FFT analysis, STFT analysis, and high order cumulate spectrum analysis, emphasize the frequency structure analysis of vibration signals. They aim at finding some efficient fault features from the vibration signals and have had good application in fault diagnosis. Combining these feature extraction methods with pattern recognition theories, such as neural network, GMM network, fuzzy logic network, Bayesian network, it is possible to realize intelligent on-line identification and fault diagnosis of machinery vibration signals [1-6]. However, these methods have shortcomings as they are more concerned about the frequency domain rather than

the energy distribution and structural features. It is still a challenge to explore effective techniques that can extract specific features from vibration signals.

Vibration signals from hydropower stations usually demonstrate unstable and transient properties. Some are even random variation signals, and these signals show fractal features to some extent. The analysis of vibration signals has evolved with the development of the signal-processing method. Traditional fractal theory has been used in the fault diagnosis of hydropower units in recent years, and proved to be feasible^[7-8]. It provides a geometric structure analysis method for complex signals, and has a number of successful applications in many fields. For example, chaotic fractal theory has been applied to the feature extraction of fault diagnosis of gas valves in [9] and a three-dimensional fractal measurement for a rock joint surface was conducted, and studied the relationship between surface fractal characteristic and hydro-mechanical behavior was studied in [10]. In fault diagnosis of mechanical equipment, fractal geometry method is used in vibration signal analysis with some fruitful outputs in [11]. However, there's still some significant disadvantages in traditional methods. One widely used method of conventional fractal theory is GP method in calculating the correlation dimension. However, signal features can't be described adequately by the method for it only reflects the irregularity of signal as a whole, thus leading to the lack of local singularity description^[23]. The recently

developed wavelet fractal algorithm, however, satisfies the requirement of local singularity description as well as reflects the whole irregularity of signal.

The wavelet fractal algorithm has proven particularly applicable in the feature extraction of vibration signals^[12]. However, its application is only found in the field of rotating machinery for its novelty. Considering the similarity between hydro-turbine vibration signals and rotating machinery vibration signals, it is felt that the wavelet fractal algorithm might be also applicable in the field of hydropower units. The principle of fractal-wavelet spectrum is simple: decompose vibration signals into different frequency components, then calculate the variance of each frequency band individually, which describes the energy distribution on each level, so as to describe the complexity and irregularity of signal on different scales and frequency bands. Wavelet fractal algorithm on several sets of simulated hydro-power vibration signals is conducted in this paper in two steps: first draw the power spectrum of the de-noised signal for the chosen wavelet function and decomposition level used in the algorithm; then decompose the signal and calculate the variance of selected decomposed levels, thus acquiring the fractal dimension after a few simple mathematical steps. For comparison, conventional fractal dimension calculating algorithm is also applied on the same set of data. The results show that although both methods are successful in feature extraction, the proposed wavelet fractal algorithm shows better performance in accuracy.

2. Fractal dimension and GP method

2.1 Fractal dimension

Non-linear dynamic and chaotic theory can be used to describe the irregular, broadband signals, which are generic in non-linear dynamic systems. They are effective in extracting some physically interesting and useful features from such signals. Fractal dimension, the capacity dimension, correlation dimension, and information dimension,—developed from the non-linear dynamic and chaotic theory, is a promising new tool to interpret observations of physical systems with a fractal structure^[12].

2.2 Definition of fractal dimension

There are quite a few classifications of fractal dimension: self-similarity dimension, Hausdorff dimension, box dimension, correlation dimension, information dimension, etc. The definition of fractal dimension differs as the classification changes^[13]. In spite of the differences in the manner of their definitions, the essence is the same: measure the fractal diagram or signal on a certain scale, then express fractal dimension

as the ratio of measuring result to the measuring scale. For instance, the self-similarity dimension D is defined by fractal graphics with strict self-similarity as^[22]:

$$D = \lim_{\delta \rightarrow 0} \frac{\ln N}{\ln(1/r)} \quad (1)$$

Assume that the fractal entirety S consists of N non-overlapping parts $s_1, s_2, s_3, \dots, s_N$, and each s_i part is equal to the universal set S after a $1/r_i$ ($0 < r_i < 1$, $i=1,2,\dots,N$) time amplification. The strict requirements above put a narrow limitation to the range of its application.

The fractal dimension of a set S in a metric space, such as a geometric object or the phase space trajectory of a dynamic system, can be computed from several different measures. One of the most used measures is the correlation dimension. A widely used algorithm of correlation dimension is the G-P method proposed in [14].

2.3 Correlation dimension and Grassberger-Procaccia's algorithm

It is needed to estimate the dimension of an attractor \mathcal{A} which is embedded in an m -dimensional Euclidean space from a sample of N points on the attractor. That is, from the set $\{x_1, x_2, \dots, x_n\}$ with $x_i \in \mathcal{A} \subset \mathbb{R}^m$. It is suggested in [13] to measure the distance between every pair of points and then compute the correlation integral:

$$C(N, r) = \frac{1}{N(N-1)} \sum_{(i,j) \in \mathcal{A}} H(r - \|x_i - x_j\|) \quad (2)$$

where $H(x)$ is the Heaviside step function. The summation counts the number of pairs (x_i, x_j) for which the distance $\|x_i - x_j\|$ is less than a given positive number r .

The measure is obtained by considering correlations between points of a long-time series on the strange attractor. The practical calculation process of correlation dimension can be summarized as follows:

For a given one dimension time series $\{x_1, x_2, \dots, x_n\}$ with a fixed time increment τ and embedded dimension set to m , a matrix $X_{l \times m}$ is calculated by phase space reconstruction:

$$X_{l \times m} = [X_1, X_2, \dots, X_l]^T \quad (3)$$

where $X_i = \{x_i, x_{i+1}, \dots, x_{i+m-1}\}$, $i=1,2,\dots,l$, $l=N+1-m$.

Take the row vector X_i ($i=1,2,\dots,l$) of $X_{l \times m}$ as the point of reconstructed phase space. Measure the spatial correlation degree with the correlation integral $C(r)$ defined according to:

$$C(r) = \frac{1}{l^2} \sum_{i=1}^l \sum_{j=1}^l \theta(r - \|X_i - X_j\|) \quad (4)$$

where r is a fixed positive number, and $\theta(x)$ is the Heaviside function:

$$\theta(x) = \begin{cases} 1, & x \geq 0 \\ 0, & x < 0 \end{cases} \quad (5)$$

As the positive number r cannot be randomly selected because if it is too large, the corresponding function of $C(r)$ cannot describe the property of the system as all pairs will not be bigger than r . When r is reduced properly, a relationship between $C(r)$ and r may be established:

$$C(r) = r^D \quad (6)$$

where D is the correlation dimension. The solution formula of D is obtained as:

$$D = \lim_{r \rightarrow 0} \frac{\ln C(r)}{\ln r} \quad (7)$$

Therefore, when taking $\ln r$ as the horizontal axis and $\ln C(r)$ as the vertical axis, the slope of changing curve $(\ln C(r) - \ln r)$ is equal to correlation dimension D . The correlation dimension D is also partially determined by the embedded dimension m [8]. Thus, it is essential that the principle $m \geq 2k + 1$ (k meaning the dimension of the attractor) is followed in choosing the value of m , in which range D has been proven to be stable at a certain number without being influenced by the change of m .

3. Fractal wavelet algorithm

3.1 Feasibility of fractal-wavelet combination

Wavelet analysis is a systemic method that adopts the local dependence on the entirety, while fractal theory determines the overall signal features through studying local signal. Increasing number of studies make people realize that there is a close relationship between wavelet transform and fractal theory.

Fractal theory indicates that self-similarity (both strict and statistical self-similarity) exists among the components and the whole system. According to fractal theory, the set F generated from function $\beta(t)$ with short support is in the following form:

$$\beta(rt) = r^H \beta(t), r, H > 0 \quad (8)$$

where r is the self-similarity affine operator, H is a dimension-related parameter.

Generated from flexing and translating the mother wavelet $\psi(t)$, the family of wavelet functions $|\psi_{a,b}(t)|$ can be described as follows:

$$\psi_{a,b}(t) = |a|^{-1/2} \psi\left(\frac{t-b}{a}\right), a, b \in \mathbb{R}, a \neq 0 \quad (9)$$

where a is scaling factor, and b is displacement factor.

By comparing Eq. (8) and Eq. (9), it is not difficult to figure out that the self-similarity affine operator r and the scaling factor a are consistent, which indicates that similarity exists between fractal and wavelet theory. The consistency in cognitive process and resemblance in the essence of wavelet and fractal theory ensures the feasibility of fractal wavelet combination theory.

3.2 Fractal wavelet algorithm

Till now, fractal theory has been widely used in the description of special objects. For example, the usage of describing the time series signal with white noise and Brownian motions is becoming increasingly common [13, 14, 15]. The signals with white noise and Brownian motions are typical $1/f$ process [16]. $1/f$ process model has been successfully used in the study of physics, biology, etc. The power spectrum density function of $1/f$ process demonstrates the relationship below [13, 14, 15]:

$$S(\omega) \propto \frac{\sigma^2}{|\omega|^\beta} \quad (10)$$

where ω is angular frequency, σ^2 represents the variance of the original signal. β stands for the spectral component parameter, which represents the slope of the fitting straight line fitted from the power spectrums of different frequency band. Specifically, β equals to 1 for white noise and 2 for Brownian motion [17]. There's a relationship between the parameter H which describes self-similarity property of signals and β [18]:

$$H = \frac{\beta-1}{2} \quad (11)$$

For one-dimension signal:

$$D = 2 - H \quad (1 < D < 2, 0 < H < 1) \quad (12)$$

So it can be inferred that the relation between β and D is:

$$D = \frac{5-\beta}{2} \quad (13)$$

Not being the strict $1/f$ process, mechanical vibration has quite a lot of similarity in the aspect of typical property of nonlinear and fractal characteristic. The power spectrum of $1/f$ process centralizes on the low-frequency band, while the power spectrum of hydro-turbine unit's fault vibration signal spreads over the low and mid-high frequency band. The power spectrum of the vibration signal is as follows:

$$S(\omega_0 - \omega) \propto \frac{\sigma^2}{(\omega_0 - \omega)^\beta}, (0 < \omega < \omega_0) \quad (14)$$

$$S(\omega - \omega_0) \propto \frac{\sigma^2}{(\omega - \omega_0)^\beta}, (\omega_0 > \omega) \quad (15)$$

where ω_0 is peak center of power spectrum. Comparing the fault vibration signals' power spectrum with that of a strict $1/f$ process, there is a similarity in the form of the relationship and the difference only lies in a frequency shift.

In the fractal wavelet algorithm, the range of each frequency band is determined by the wavelet decomposition. After decomposition by orthogonal wavelet, the range for each level of detailed composition component d_{2j} is:

$$\frac{f_s}{2^{j+1}} < \omega < \frac{f_s}{2^j} \quad (16)$$

where f_s is the sampling frequency.

The power spectrum after wavelet decomposition is:

$$\frac{\sigma_l^2}{|\omega|^\beta} \leq S(\omega) \leq \frac{\sigma_h^2}{|\omega|^\beta}, 0 < \sigma_l^2 \leq \sigma_h^2 < \infty \quad (17)$$

Furthermore, the $S(\omega)$ for the signal with zero-mean can be represented by the variance of j level detailed composition component d_{2j} , denoted as $Var(d_{2j})$. Its not hard when dealing with the continuous signal $x(t)$ to make it zero mean by simply removing the average from the original signal during preprocessing. The power spectrum is the Fourier transform of self-similarity function of the signal, and it satisfies the relationship below:

$$\begin{cases} S(\omega) = \int_{-\infty}^{+\infty} R(\tau) e^{-i\omega\tau} d\tau \\ R(\tau) = \int_{-\infty}^{+\infty} S(\omega) e^{i\omega\tau} d\omega \end{cases} \quad (18)$$

where $S(\omega)$ is the power spectrum and $R(\tau)$ is the self-similarity function. So the variance of the signal is represented in the form:

$$\begin{aligned} Var[x(t)] &= E[x(t) - m_x]^2 = E[x(t)^2] \\ &= E[(x(t) - m_x)(x(t + \tau) - m_x)]|_{\tau=0} \end{aligned}$$

$$\begin{aligned} &= R(\tau)|_{\tau=0} = \int_{-\infty}^{+\infty} S(\omega) e^{i\omega\tau} d\omega|_{\tau=0} \\ &= \int_{-\infty}^{+\infty} S(\omega) d\omega \end{aligned} \quad (19)$$

The integral operator \int and the expectation operator E for continuous signal $x(t)$ corresponds to the summation operation and average operation for the discrete signal $x(n)$, respectively. So the variance and power spectrum are equivalent for zero-mean discrete signal $x(n)$ as they both measure the energy of the signal:

$$Var[x(n)] = \sum_{-\infty < \omega < +\infty} S(\omega) \Delta\omega \quad (20)$$

Therefore:

$$Var[x(n)] \propto \frac{\sigma^2}{(2^j)^\beta} \quad (21)$$

where β is the slope of the fitting straight line fitted from the logarithm of $Var(d_{2j})$ frequency band. The variance of detailed component d_{2j} is defined as:

$$Var(d_{2j}) = \frac{1}{N_j - 1} \sum (d_{2j} - m_{d_{2j}})^2 \quad (22)$$

where $m_{d_{2j}}$ is the average of the detailed component d_{2j} on scale j . N_j represents the sampling number of detailed component d_{2j} on scale j , which equals the sampling number of the signal to be analyzed.

The signal processing process is shown in Fig.1:

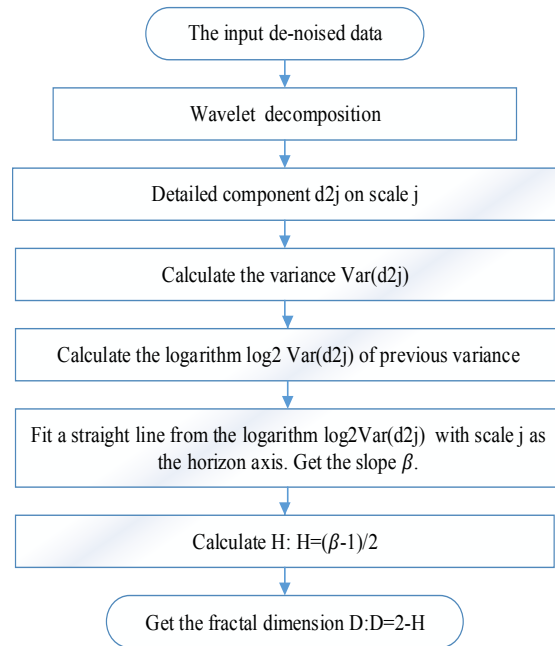


Fig.1 Signal processing process of wavelet fractal algorithm.

4. Studies and engineering applications

To verify the effectiveness of the wavelet fractal theory in the feature extraction of a hydro-turbine's vibration signals, an experiment is designed and carried out in this section.

4.1 Data acquisition

In order to assure the reliability of data used in the method, an experimental rotating machinery system is

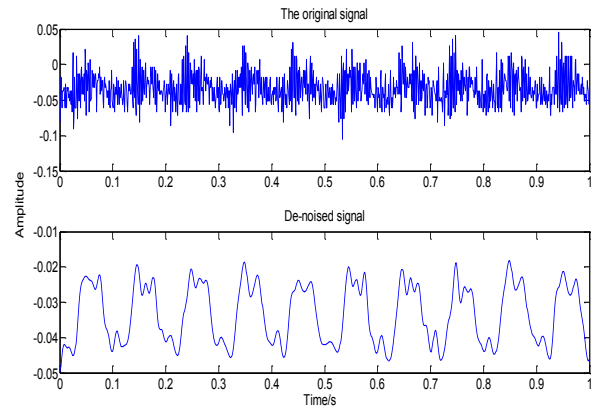
developed, and the data used in this paper is obtained from this physical system. As shown in Fig. 2, the system can simulate multiple types of rotating machinery faults. It's driven by a DC motor controlled with DH5600 speed controller. The rotor with the diameter of 10 mm and the length of 850 mm is composed of two single shafts coupled together by a coupling and supported by four bearing blocks. Two mass disks with 75 mm diameter are also fixed on the rack of the system. The sensors for signal acquisition are comprised of two eddy current sensors for displacement measurement, a photoelectric sensor for speed measurement, and a piezoelectric accelerometer for vibration measurement. The signals measured by eddy current sensors and piezoelectric accelerometer are sent to a proxymitor for filtering, amplification, and then the signals are transmitted to computer for collection and analysis.



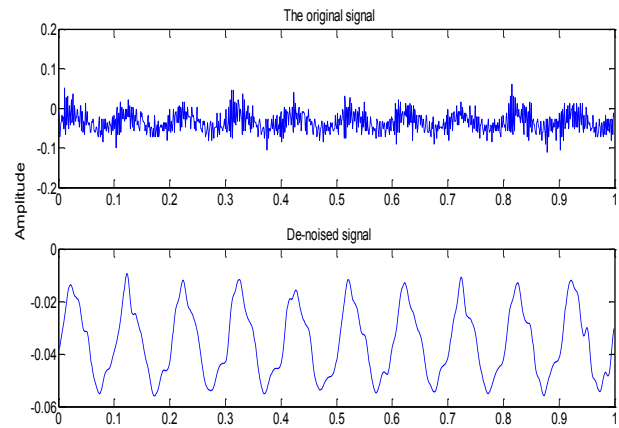
Fig.2. Experimental machinery system.

Several machine conditions are considered including normal, unbalance, and misalignment conditions. The unbalance condition is simulated by screwing a 2g mass block into the threaded hole near the edge of the mass disk 1, while the misalignment condition is simulated by misaligning the coupling of the rotor. During the process of experimentation, speed of the system is assigned to 1200 rpm, and the sampling frequency is 2048 Hz. Under each of the three conditions, 30 vibration files with 2048 points are acquired for calculating and comparing two feature extraction methods introduced above. One group of original data is shown in Fig. 3.

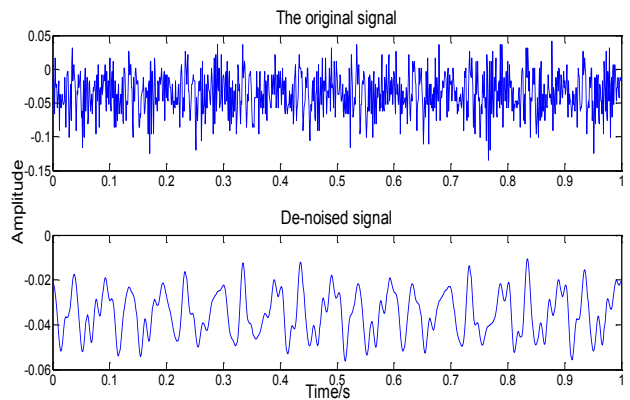
It can be seen from Fig.3 that the original signals are submerged in substantial noises, thus their characteristics are blurred. Therefore, it is important to apply signal de-noising before conducting feature extraction on the signals. The signal de-noising method applied in this paper is wavelet transform de-noising^[19].



a) The original and de-noised signal under normal condition.



b) The original and de-noised signal under unbalanced condition.



c) The original and de-noised signal under misalignment condition

Fig.3 the original and de-noised signals under different conditions.

4.2 Feature extraction

4.2.1 Feature extraction by fractal theory with GP method

A generally used fractal dimension algorithm is introduced in section 2.3. Grassberger-Procaccia's (GP's) algorithm is widely used in acquiring the fractal dimension for its reliability and simplicity of calculation. The key parameters of the GP method are the reconstruction phase space dimension m , time delay τ , and the positive scalar r . Adaptive improvements have been made to the method, like the principle in the selection of reconstructed phase space's dimension, the value of the positive number r . There are some principles to follow when applying GP method to the calculation of the fractal dimension of fault vibration signals:

i) The reconstruction phase space dimension m should satisfy: $m \geq 2d + 1$, suggesting the attractor of the original signal exists in a d -dimensional space.

ii) The selection of τ . If τ is too small, the outcome curve would shrink to the same direction in space; if the value is too large, distortion would occur in the phase diagram. The Rosenstein's recommended value^[20] is adopted in this article, where $\tau = \frac{1}{\epsilon} L$, L is the initial value of the auto-correlation function.

iii) The range of r . Studies and research suggest that the upper limit should be set to the value where $\ln C(r)$ is approximately zero, and the lower limit equals the value where the fractal dimension D is close to the phase space dimension m .

Following the principles suggested above, feature extraction is conducted on the experimental data. Figs 4 (a)-(c) demonstrate the double logarithmic curves on different fault situations. The scale-free interval of each figure is marked on it. There are several curves in each figure, corresponding to different values of phase space dimension m . Although the curves don't overlap, curve-segments within the scale-free interval are similar to straight lines and they are parallel with each other. The slope of the curve-segment is the fractal dimension D . For each of the three fault conditions, 30 sets of data were required. Results are listed in Fig. 5.

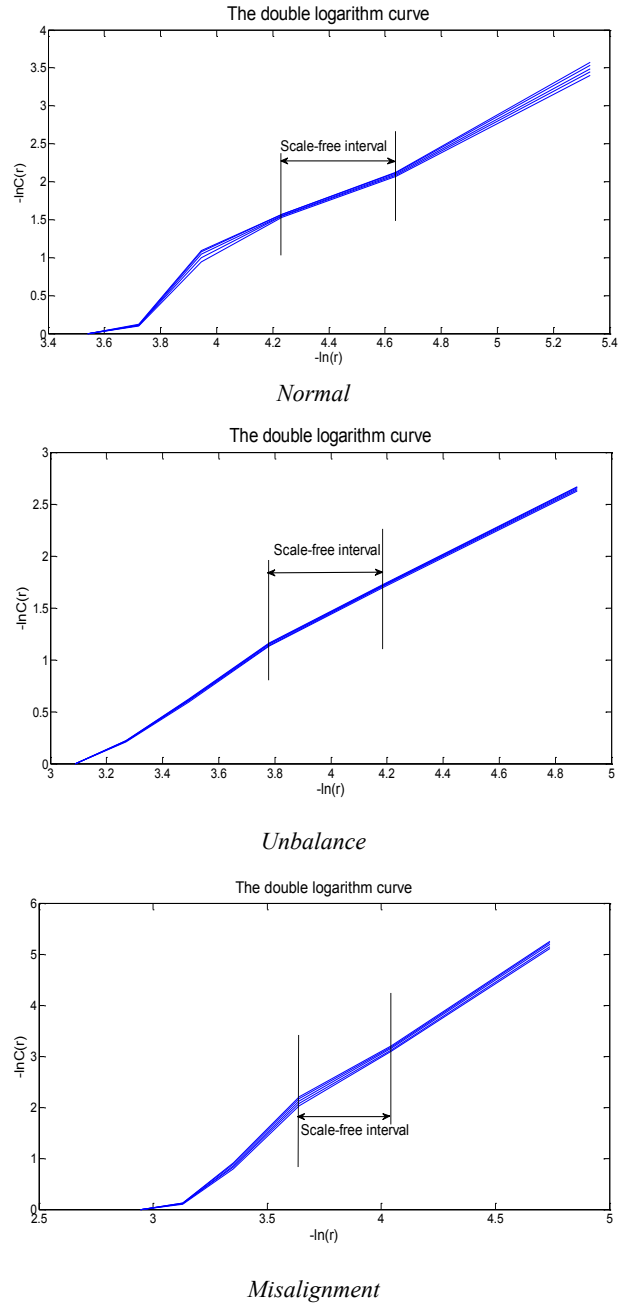


Fig.4. Double logarithm curves for different conditions.

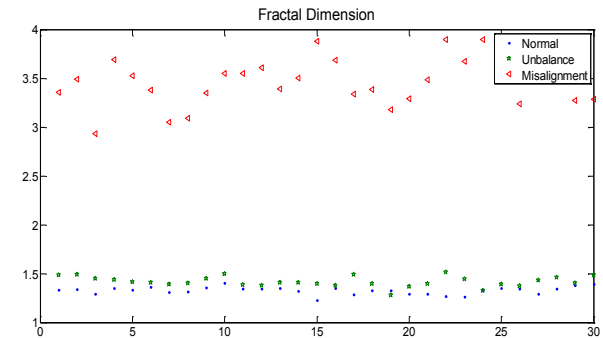


Fig.5. Fractal dimension of different conditions using GP method.

4.2.2 Feature extraction by wavelet fractal spectrum

As shown in Fig.3, vibration signals under different circumstances are acquired from the lab and have been de-noised. The rotational speed of the experimental system is set to 1200 rpm, and the sampling frequency is 2048 Hz. In order to choose the wavelet function used in the method, the power spectrum of the experimental data is required. Figs 6 (a)~(c) show the power spectrum under normal, unbalance and misalignment conditions, respectively. For a clearer view, the spectrum with frequency over 200 Hz and zero amplitude is neglected in these figs.

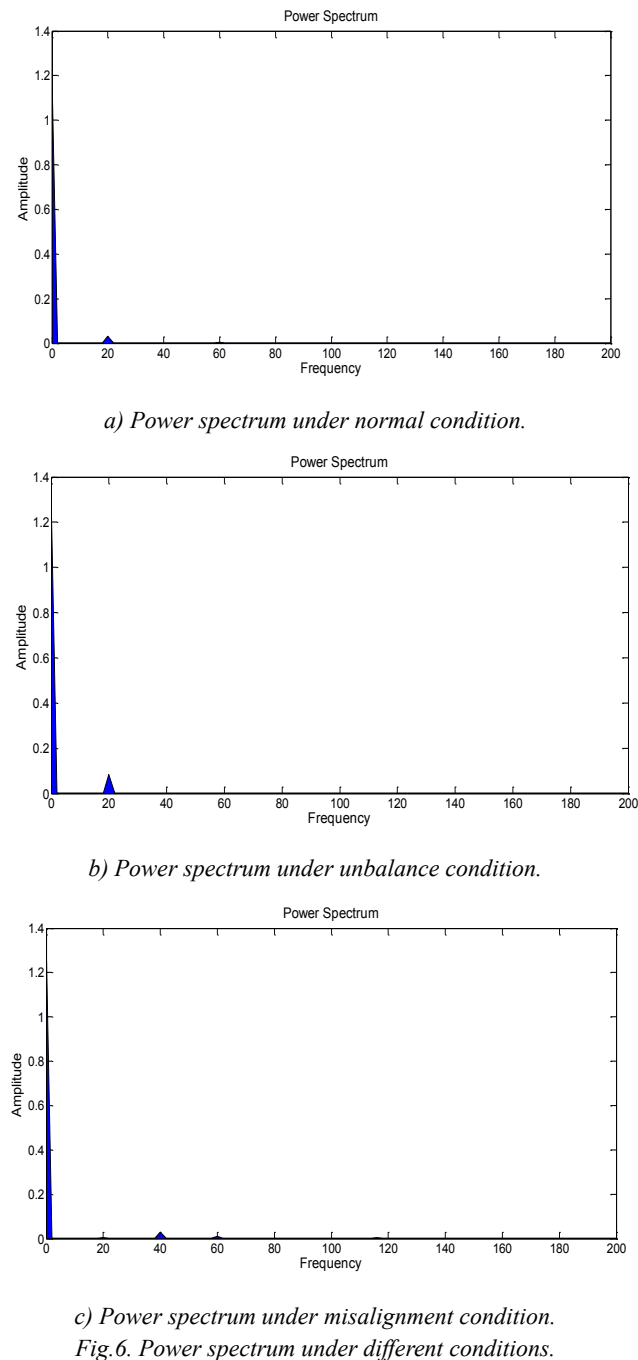
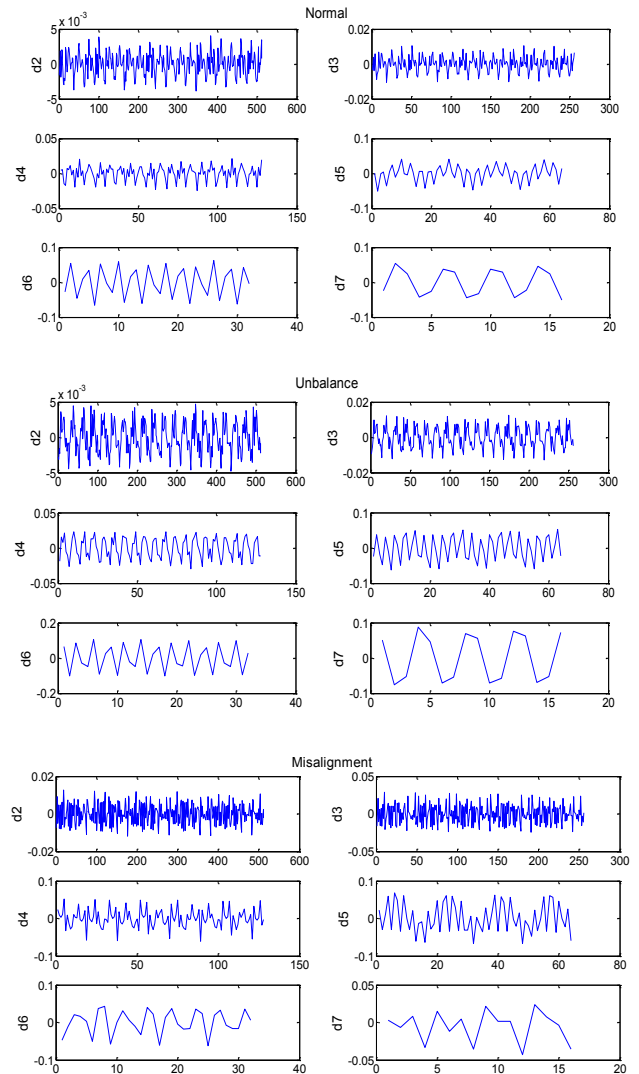
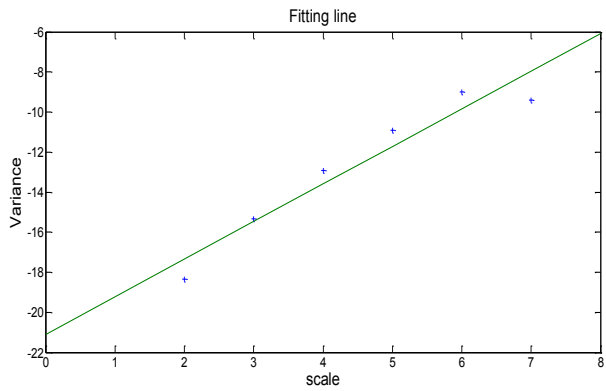


Table 1. Decomposed frequency bands and corresponding frequency range.

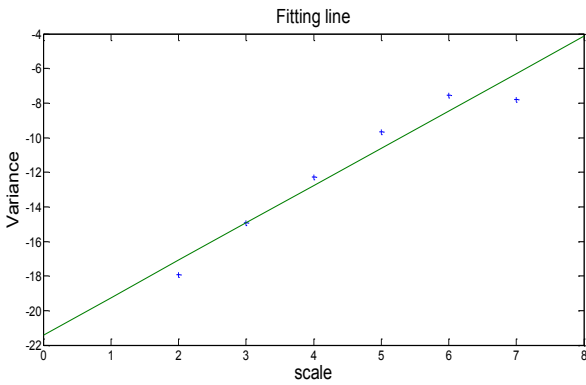
Level	1	2	3	4	5	6	7	8
Frequency range/Hz	1024	512	256	128	64	32	16	8
	-	-	-	-	-	-	-	-
	2048	1024	512	256	128	64	32	16

Table 1 shows the decomposed frequency bands and their range of wavelet function 'db8' when the decomposition level is set to 8, corresponding to 8 bands. The spectrum of different conditions differs in tiny details, and the overall feature of power spectrums shown in Fig. 6 is that the energy of the signals concentrates in the range of 0 to 60 Hz. The detail components on levels 2 to 7, Table 1, contain the majority of total energy as seen in Fig. 7 for different conditions. So they are occupied in calculating the fractal dimension. The fitted straight lines under different conditions taking scale j as the horizontal axis and the variance $Var(d_j)$ of each level as the vertical axis, are shown in Fig. 8.

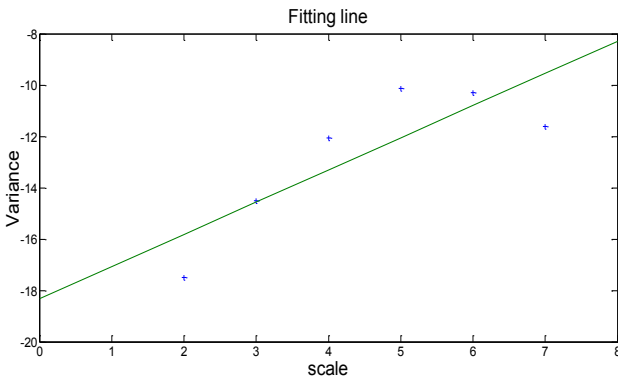




a) Fitting line under normal condition.



b) Fitting line under unbalance condition.



c) Fitting line under misalignment condition.

Fig.8 Fitting lines under different conditions.

For each of the three fault conditions, 30 sets of data were acquired. Taking the de-noised signals as the input data to the wavelet fractal algorithm, the fractal dimensions can be obtained. The obtained fractal dimension is shown in Fig. 9.

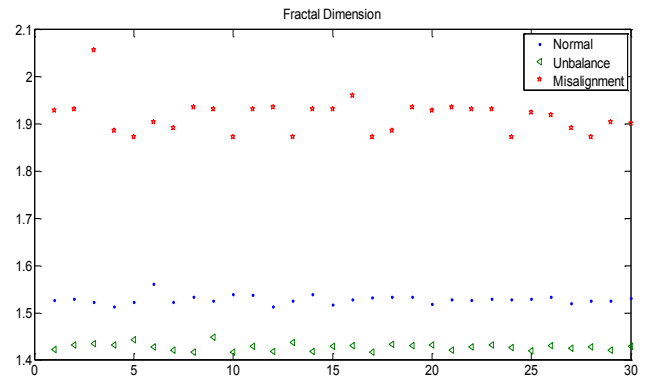


Fig.9. Fractal dimension of different conditions using wavelet fractal algorithm.

4.3 Analysis and comparison

Two methods of feature extraction using fractal dimension in fault diagnosis of hydro-turbine units are introduced. In this section, an experimental verification is conducted. Figs. 5 and 9 are the outcomes of conventional correlation dimension algorithm and novel wavelet fractal algorithm, respectively. It can be seen that both methods are successful in feature extraction. However, more clutter is demonstrated in Fig. 5 and there are overlaps between the fractal dimensions under normal and unbalanced conditions, while the fractal dimensions in Fig. 9 shows clear boundaries among three conditions. For a better illustration, statistical parameters of both algorithms are calculated and are listed in Table. 2.

Table 2. Statistical parameters of results using different algorithms.

Algorithm Condition	GP method		Wavelet fractal theory	
	Average	Standard deviation	Average	Standard deviation
Normal	1.3267	0.0379	1.5286	0.0089
Unbalance	1.4184	0.052	1.4280	0.00749
Misalignment	3.484	0.261	1.9163	0.0366

The reason for the difference in average even under the same condition is due to the essence of the methods. The GP method considers the absolute fractal dimension of the signals, whereas the essence of the wavelet fractal theory is to investigate the relative distribution of energy on different scales under various conditions, that is, the relative distribution of power spectrum on different frequency bands. Thus, the fractal dimensions acquired from wavelet fractal algorithm is a relative value. The standard deviation of wavelet fractal theory is much smaller than that of the GP method, which indicates the superiority of the wavelet fractal algorithm in the aspect of accuracy.

4.4 Engineering application

We managed to get a set of normal condition data and fault vibration data from a hydropower plant in China. The structure of its power generator is demonstrated in Fig.10. The power generator were noticed on a certain day to be vibrated so intensely that the amplitude of the vibration signals exceeded the safety threshold. After a series of examination and test, the experts diagnosed the fault pattern as unbalance fault. After performing counterweight process to the power generator, the amplitude of the vibration signals returned to normal.

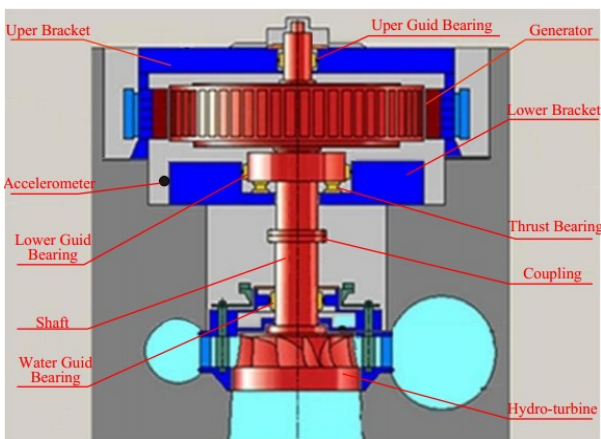
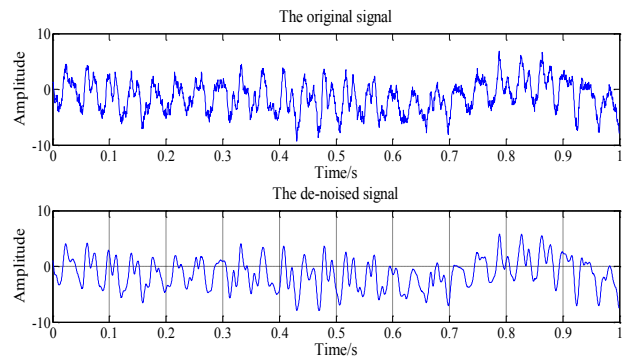
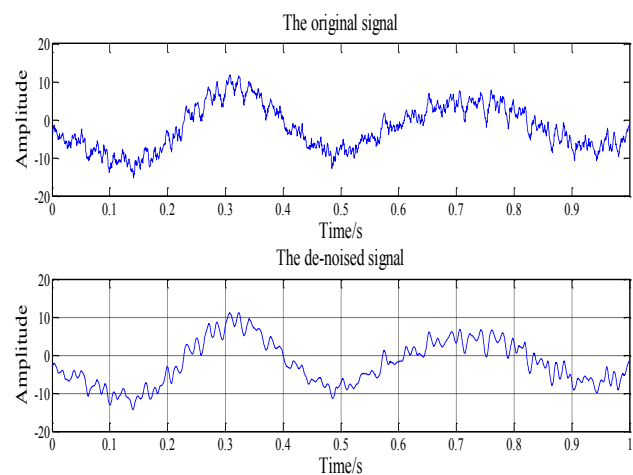


Fig.10. Sketch of the power generator structure.

The signal acquired before and after the counterweight are taken as signals under unbalance and normal conditions, respectively. During the process of operation, the speed of the power generator was 500 rpm, and the sampling frequency was 500Hz. Under each of the two conditions, 25 sets of vibration data with 512 points in each are acquired and de-noised as shown in Fig.11, feature extracted with wavelet fractal algorithm.



a) The original and de-noised signal under normal condition.



b) The original and de-noised signal under unbalance condition.

Fig.11. The original and de-noised signal under different conditions

The feature extraction process using wavelet fractal algorithm is the same as described in section 3. Taking the de-noised signals as the input of the process shown in Fig.1, vibration signals under normal and unbalance conditions are feature extracted respectively, 25 sets of data under each condition. Result is demonstrated as follows.

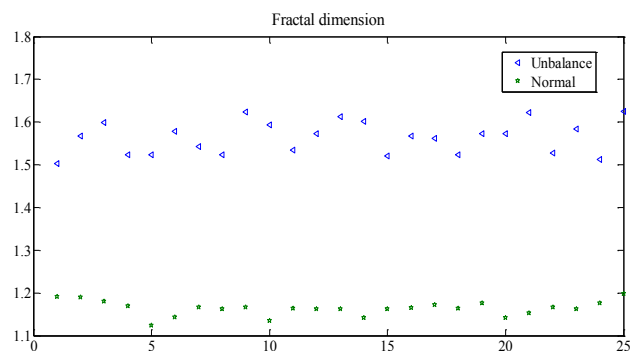


Fig.12. Fractal dimension of different conditions using wavelet fractal algorithm.

The fractal dimension under normal and unbalance condition divided into two groups with a clear boundary, confirming the effectiveness of the proposed feature extraction algorithm. However, the standard deviations of each condition's fractal theory are quite big comparing to those of the experiment. The reason is that the field test data acquired from hydropower station contains more information of its surrounding field conditions which would influence the vibration signals significantly in comparison with the experiment signals. The engineering application is a strong verification for the effectiveness of the proposed algorithm in feature extraction in fault diagnosis of hydropower vibration signals.

5. Conclusions

Recently, fractal theory and dimension have been developed and applied to fault diagnosis in many fields, including the fault diagnosis of hydro-turbine units. However, the fractal theory does not include the detail components of acquired signals, which may cause deviation in diagnosis. A wavelet fractal spectrum algorithm is developed in this paper by combining fractal theory with wavelet decomposition. The proposed method along with the correlation dimension acquired from GP method is applied to feature extraction of signals measured from experiments under three different conditions. Both methods show success in extracting features from signals under different conditions. By comparing the statistical parameters of the two methods, it can be inferred that the feature extracted with wavelet fractal spectrum algorithm has higher accuracy and thus this algorithm provides a more accurate feature extraction method in the fault diagnosis of hydro-turbine units.

Acknowledgement

The authors acknowledge the financial support from the National Natural Science Foundation of China under Grant No.51379160

References

- [1] T.B. Brotherton, T. Pollard, Proceeding of IEEE Signal Processing International Symposium on Time-Frequency and Time-Scale Analysis. Orlando, FL, **2242**, 95 (1992).
- [2] H.C. Choe, C.E. Poole, A.M. Yu, Proceedings of the SPIE Wavelet Applications, **2419**, 504 (1995).
- [3] D.M. Yang, A.F. Stronach, P. MacConnel, Mechanical Systems and Signals processing, **16**(2-3), 391 (2002).
- [4] J.A. Leonard, M.A. Kraner, Radial basis function networks for classifying process faults[J]. IEEE Control Systems Magazine, p. 31, 1991.
- [5] Chow, R.N. Sharpe, J.Hung, IEEE Transaction on Industrial Electronics, **40**(2), 189 (1993).
- [6] L.P. Heck, K.C. Chou, Proceedings of the IEEE world Congress on Computational Neural Network and International Conference on Intelligence, **7**, 4493 (1994).
- [7] Peng Zhike, He Yongyong, Lu Qing, Chinese journal of mechanical engineering, **38**(8), 59 (2002).
- [8] Li Yongqiang, Liu Jie, Chinese journal of applies mechanics, **24**(2), 302 (2007).
- [9] Ma Jin, Jiang Zhinong, Gao Jinji, Journal of vibration and shock, **31**(19), 26 (2012).
- [10] Y.J. Jiang, Y. Tanabashi, K. Nagaie, Relationship between surface fractal characteristic and hydro-mechanical behavior of rock joints[C]. Proceedings of the ISRM International Symposium 3rd ARMS, Ohnishi & Aoid, 2004.
- [11] S. Edward, A.W. Lees, M.I. Friswell, Shock and vibration digest, **30**(1), 4 (1998).
- [12] Mandelbrot, B. Benoit, The Fractal Geometry of Nature[M]. San Francisco: W.H.Freeman, 1982.
- [13] Falconer K.J. Fractal geometry: Mathematical foundation and applications[M]. Chichester: John Wiley & Sons Ltd, 1990.
- [14] Weiguo Huang, Research On Feature Extraction and Representation with Vibration signal for rotary Machinery Condition Monitoring and Fault Diagnosis[D], 2010.
- [15] P. Grassberger, I. Procaccia, Physica D, **9**, 189 (1983).
- [16] W.G. Wornell, A.V. Oppenheim, IEEE Trans. Signal Proceeding, **40**, 611 (1992).
- [17] Flandrin, IEEE Trans. Inform. Theory, **35**, 197 (1989).
- [18] Flandrin.P., IEEE Trans. Inform. Theory, **38**(Part 2), 910 (1992).
- [19] B.B. Mandelbort, H.W. Van Ness, SIAM Rev, **10**, 422 (1968).
- [20] Su Li, Nan Haipeng, Yu Xiangyang, et al. Journal of Hydroelectric engineering, **31**(3), 246 (2012).
- [21] M. Hoschneider. Communications in Mathematical Physics, **160**(3), 457 (1994).
- [22] Jizhong Zhang. Fractal[M]. Beijing: Tsinghua University Press, p. 23, 1997.
- [23] Li Tong, Multifractal theory and some applications[D].Beijing Jiaotong University, p. 6, 2008.

*Corresponding author: xiaozhihuai@126.com